



113/295/DTS

DRAFT TECHNICAL SPECIFICATION

Project number	IEC TS 62607-6-4 Ed. 1.0	
IEC/TC or SC 113	Secretariat Germany	
Distributed on 2015-12-18	Voting terminates on 2016-03-18	

Also of interest to the following committees ISO/TC 229	Supersedes document 113/269/CD and 113/294/CC		
Functions concerned			
<input type="checkbox"/> Safety	<input type="checkbox"/> EMC	<input type="checkbox"/> Environment	<input type="checkbox"/> Quality assurance

THIS DOCUMENT IS STILL UNDER STUDY AND SUBJECT TO CHANGE. IT SHOULD NOT BE USED FOR REFERENCE PURPOSES.

RECIPIENTS OF THIS DOCUMENT ARE INVITED TO SUBMIT, WITH THEIR COMMENTS, NOTIFICATION OF ANY RELEVANT PATENT RIGHTS OF WHICH THEY ARE AWARE AND TO PROVIDE SUPPORTING DOCUMENTATION.

Title

IEC 62607-6-4: Nanomanufacturing – Key control characteristics – Part 6-4: Graphene - Surface conductance measurement using resonant cavity

Copyright © 2015 International Electrotechnical Commission, IEC. All rights reserved. It is permitted to download this electronic file, to make a copy and to print out the content for the sole purpose of preparing National Committee positions. You may not copy or "mirror" the file or printed version of the document, or any part of it, for any other purpose without permission in writing from IEC.

CONTENTS

1		
2		
3	FOREWORD	3
4	INTRODUCTION	5
5	1 Scope	6
6	2 Normative references	6
7	3 Terms and definitions	6
8	4 Microwave cavity test fixture	8
9	5 Test Specimen	9
10	6 Measurement procedure	9
11	7 Calculations of surface conductance	10
12	8 Report	11
13	9 Notes	11
14	10 Accuracy Consideration	12
15	Annex A (informative) Case study of surface conductance measurement of SL and ML graphene	
16	13
17	A.1 General	13
18	A.2 Cavity Perturbation Procedure	13
19	A.3 Experimental	14
20	A.4 Results	14
21	A.5 Surface conductance of SL and ML graphene	15
22	A.6 Summary	15
23	Bibliography	16
24		
25	Fig. 1 - Microwave cavity test fixture. (1) waveguide, (2) couplers, (3) slot for specimen insertion,	
26	(4) specimen, (5) specimen holder.	9
27	Figure A.1 – Scattering parameters $ S_{21} $ of the resonant peak TE_{103} as a function specimen	
28	insertion (h_x).	14
29	Fig A.2 – Plots of $(1/Q_x - 1/Q_0)$ as a function of the normalized specimen area, wh_x , for (SL) and	
30	(ML) CVD graphene.	15
31		
32		

INTERNATIONAL ELECTROTECHNICAL COMMISSION

NANOMANUFACTURING – KEY CONTROL CHARACTERISTICS –
Part 6-4: Graphene - Surface conductance measurement using resonant cavity

FOREWORD

- 1) The International Electrotechnical Commission (IEC) is a worldwide organization for standardization comprising all national electrotechnical committees (IEC National Committees). The object of IEC is to promote international co-operation on all questions concerning standardization in the electrical and electronic fields. To this end and in addition to other activities, IEC publishes International Standards, Technical Specifications, Technical Reports, Publicly Available Specifications (PAS) and Guides (hereafter referred to as "IEC Publication(s)"). Their preparation is entrusted to technical committees; any IEC National Committee interested in the subject dealt with may participate in this preparatory work. International, governmental and non-governmental organizations liaising with the IEC also participate in this preparation. IEC collaborates closely with the International Organization for Standardization (ISO) in accordance with conditions determined by agreement between the two organizations.
- 2) The formal decisions or agreements of IEC on technical matters express, as nearly as possible, an international consensus of opinion on the relevant subjects since each technical committee has representation from all interested IEC National Committees.
- 3) IEC Publications have the form of recommendations for international use and are accepted by IEC National Committees in that sense. While all reasonable efforts are made to ensure that the technical content of IEC Publications is accurate, IEC cannot be held responsible for the way in which they are used or for any misinterpretation by any end user.
- 4) In order to promote international uniformity, IEC National Committees undertake to apply IEC Publications transparently to the maximum extent possible in their national and regional publications. Any divergence between any IEC Publication and the corresponding national or regional publication shall be clearly indicated in the latter.
- 5) IEC itself does not provide any attestation of conformity. Independent certification bodies provide conformity assessment services and, in some areas, access to IEC marks of conformity. IEC is not responsible for any services carried out by independent certification bodies.
- 6) All users should ensure that they have the latest edition of this publication.
- 7) No liability shall attach to IEC or its directors, employees, servants or agents including individual experts and members of its technical committees and IEC National Committees for any personal injury, property damage or other damage of any nature whatsoever, whether direct or indirect, or for costs (including legal fees) and expenses arising out of the publication, use of, or reliance upon, this IEC Publication or any other IEC Publications.
- 8) Attention is drawn to the Normative references cited in this publication. Use of the referenced publications is indispensable for the correct application of this publication.
- 9) Attention is drawn to the possibility that some of the elements of this IEC Publication may be the subject of patent rights. IEC shall not be held responsible for identifying any or all such patent rights.

International Technical Specification IEC 62607-6-4 has been prepared by IEC technical committee 113.

The text of this standard is based on the following documents:

FDIS	Report on voting
113/XX/FDIS	113/XX/RVD

Full information on the voting for the approval of this standard can be found in the report on voting indicated in the above table.

This publication has been drafted in accordance with the ISO/IEC Directives, Part 2.

79 The committee has decided that the contents of this publication will remain unchanged until the stability
80 date indicated on the IEC web site under "<http://webstore.iec.ch>" in the data related to the specific
81 publication. At this date, the publication will be

- 82 • reconfirmed,
- 83 • withdrawn,
- 84 • replaced by a revised edition, or
- 85 • amended.

86

87 The National Committees are requested to note that for this publication the stability date is 20XX.

88 THIS TEXT IS INCLUDED FOR THE INFORMATION OF THE NATIONAL COMMITTEES AND WILL BE DELETED AT THE
89 PUBLICATION STAGE.

90

91

INTRODUCTION

92 The microwave resonant cavity test method for surface conductance is non-contact, fast, sensitive and
93 accurate. It is well suited for standards, research and development (R&D), and for quality control in
94 the manufacturing of two-dimensional (2D) nano-carbon graphene materials. These sheet-like or flake
95 like nano-carbon carbon forms can be assembled into atomically-thin monolayer or multilayer
96 graphene materials, which can be stacked, folded, crumpled or pillared into a variety of nano-carbon
97 architectures with the lateral dimension limited to few tenths of a nanometer. Many of these materials
98 are new and exhibit extraordinary physical and electrical properties such as optical transparency,
99 anisotropic heat diffusivity and charge transport that are of significant interest to science, technology
100 and commercial applications [1, 2].

101

102

103 Depending on particular morphologies, density of states and structural perfection, the surface
104 conductance of these materials may vary from 1 S to about 10^{-4} S. Conventional direct current (DC)
105 surface conductance measurement techniques require a complex test vehicle and interconnections for
106 making electrical contacts, which affect and alter the measurement, making it difficult to decouple the
107 intrinsic properties of the material.

108

109 In comparison, resonant cavity measurement method is fast and non-contact. Thus, it is well suited for
110 use in R&D and manufacturing environments where the surface conductance is a critical functional
111 parameter. Moreover, it can be employed to measure electrical characteristics of other nano-size
112 structures.

113

114

115

NANOMANUFACTURING – KEY CONTROL CHARACTERISTICS –

Part 6-4: Graphene - Surface conductance measurement using resonant cavity

1 Scope

This part of IEC 62607 establishes a method for determining the surface conductance of 2D single-layer or multi-layer atomically thin nano-carbon graphene structures. These are synthesized by chemical vapour deposition (CVD), epitaxial growth on silicon carbide (SiC), obtained from reduced graphene oxide (rGO) or mechanically exfoliated from graphite. The measurements are made in an air filled standard R100* rectangular waveguide configuration, at one of the resonant frequency modes, typically at 7 GHz.

Surface conductance measurement by resonant cavity involves monitoring the resonant frequency shift and change in the quality factor before and after insertion of the specimen into the cavity in a quantitative correlation with the specimen surface area. This measurement does not explicitly depend on the thickness of the nano-carbon layer. The thickness of the specimen does not need to be known, but it is assumed that the lateral dimension is uniform over the specimen area.

2 Normative references

The following documents, in whole or in part, are normatively referenced in this document and are indispensable for its application. For dated references, only the edition cited applies. For undated references, the latest edition of the referenced document (including any amendments) applies.

For the purposes of this document, the terms and definitions given in publications listed below and the following terms and definitions apply.

ISO/IEC TS 80004-13, *Nanotechnologies – Vocabulary – Part 13: Graphene and other two-1 dimensional materials*

IEC 62565-3-1 (113/247/CD), *Nanomanufacturing – Material Specifications – Part 3-1: Graphene - Blank detail specification for electrotechnical applications*

IEC 60153-2, *Hollow metallic waveguides – Part 2: Relevant specifications for ordinary rectangular waveguides*

NOTE In some countries the R100 standard waveguide is referenced as WR-90

3 Terms and definitions

3.1 Graphene Layers

Single graphene layer (SLG)

a single atom-thick sheet of hexagonally arranged, bonded carbon atoms with sp^2 -electronic hybridization in a honeycomb structure.

NOTE: SLG is an important building block of many carbon nano-objects.

Bilayer graphene, trilayer graphene (BLG, TLG)

2D (sheet-like) materials, either as free-standing films or flakes, or as a substrate-bound coating, consisting of 2 or 3 well-defined countable, stacked graphene layers of extended lateral dimension.

157

158 Multi-layer graphene (MLG)

159 a 2D (sheet-like) material, either as a free-standing flake or substrate-bound coating, consisting of a
160 small number (4-10), stacked graphene layers of extended lateral dimension.

161 Graphite nanoplates

162 nanosheets, nanoflakes, 2D materials of graphite, with ABA or ABCA stacking and having a thickness
163 and/or lateral dimension less than 100 nm.

164 Graphene oxide (GO)

165 chemically modified graphene prepared by oxidation and exfoliation that is accompanied by extensive
166 oxidative modification of the basal plane. Graphene oxide is a monolayer material with a high oxygen
167 content, typically characterized by C/O atomic ratios less than 3.0 and typically closer to 2.0.

168 Reduced graphene oxide (rGO)

169 graphene oxide that has been processed to reduce its oxygen content.

170 Graphene materials

171 overarching term representative of graphene-based materials, graphene nanomaterials, graphene-family
172 nanomaterials [11] for the collection of 2D materials that contain the word “graphene”, including
173 multilayered materials (n less than about 10), chemically modified forms (GO, rGO), and materials made
174 via another precursor material or process such as chemical vapour deposition (CVD).

175 3.2 Measurement terminology

176

177 Surface Conductance

178 applicable to thin films that can be considered as two-dimensional entities having the geometrical width
179 (W) and length (L), where the charge transport takes place along the plane of the specimen layer rather
180 than perpendicular to it. When voltage (u) is applied uniformly across L , the resulting electric current (i) is
181 proportional to the surface conductance (σ_s) and the specimen width, W , while in reciprocal proportion to
182 the specimen length:

$$183 \quad G = i/u = \sigma_s (W/L)$$

184 Where:

185 σ_s = the characteristic property of 2D materials.

186 Note the SI unit of measure of σ_s is siemens (S). In the trade and industrial literature, however, siemens per square (S/square)
187 is commonly used when referring to surface conductance. This is to avoid confusion between surface conductance and electrical
188 conductance (G), which share the same unit of measure.

189 Electrical Conductance (G)

190 measure of how easily electrical current flows along a certain path.

191 NOTE The SI unit of G is siemens (S).

192 Electrical conductivity

193 characteristic physical property of 3D materials describing the ability to conduct electric current.

194 NOTE The specific volume conductance can be obtained from surface conductance dividing it by the conductor
195 thickness (t): $\sigma_v = \sigma_s/t$. The unit of measure of σ_v is siemens per meter (S/m).

196

197 Surface (sheet) resistance (ρ_s)

198 a reciprocal of σ_s , a characteristic property of 2D charge transport.

199 NOTE Sheet resistance measurements are commonly made to characterize the uniformity of conductive or semi-conductive
200 coatings for quality assurance. The SI unit of measure of ρ_s is ohm (Ω). In the trade and industrial literature, however, ohm per

201 square (S/square) is commonly used when referring to surface resistance. This is to avoid confusion between surface resistance
 202 and electrical resistance (R), which share the same unit of measure.

203

204 **Microwave Cavity**

205 also known as a radio frequency (RF) cavity, a special type of resonator consisting of a closed metal
 206 structure that confines electromagnetic fields in the microwave range of the spectrum.

207 NOTE: The structure can be filled with air or other dielectric material. A microwave cavity acts similarly to a resonant circuit with
 208 extremely low loss at its frequency of operation.

209 Microwave resonant cavities are typically made from closed (or short-circuited) sections of a waveguide. Every cavity has
 210 numerous **resonant frequencies** (f_r) that correspond to electromagnetic field modes satisfying the necessary boundary
 211 conditions i.e. the cavity length must be an integer multiple of half-wavelength at resonance.

212

213 **Quality factor (Q)**

214 a dimension-less parameter describing the ratio of energy stored in the resonant circuit to time-averaged
 215 power loss of the cavity, or equivalently, a resonator's half power bandwidth, (Δf) relative to the resonant
 216 frequency (f_r):

217

$$218 \quad Q = f_r / \Delta f$$

219

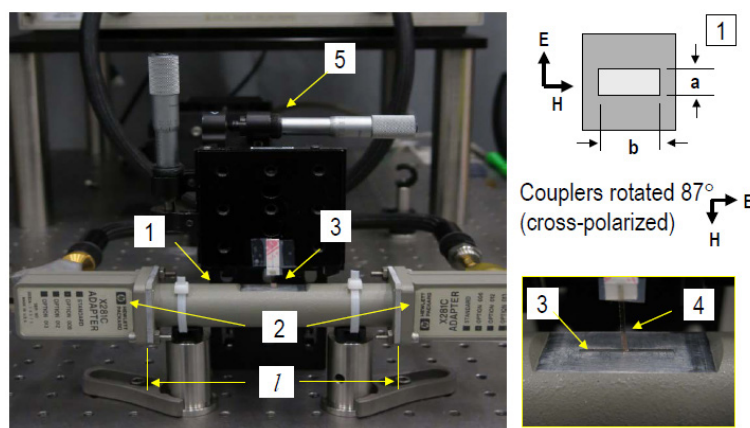
220 **Microwave scattering parameters (S-parameters) (S_{ij})**

221 Factors that quantify how RF energy propagates through a microwave multi-port network. Subscript (i)
 222 indicates the detecting port. Subscript (j) refers to the sourcing (input) port. Accordingly, S_{21} quantifies
 223 microwave energy that is transmitted from port_1 to port_2. In comparison, S_{11} quantifies microwave
 224 energy that is sourced and detected at port_1 and it is often referred as a reflection coefficient.

225 **4 Microwave cavity test fixture**

226 The test fixture is shown in Fig. 1. It consists of a R100 waveguide (1), having nominal **load impedance of**
 227 **50Ω such the Voltage Reflected Standing Wave ratio (VRSW) is 1.04:1.0 or less, and the insertion loss is less**
 228 **than 0.5 dB/m.** This waveguide can operate in the microwave frequency range of 6.6 GHz to 13 GHz. The
 229 waveguide dimensions are: $a = 10.16 \text{ mm}$, $b = 24.6 \text{ mm}$ and its length $l = 134 \text{ mm}$. The walls of the cavity
 230 are implemented via coax to R100 waveguide couplers (2), which are cross-polarized ($\theta = 87^\circ$) with
 231 respect to the waveguide electromagnetic field polarization, E and H. The resonant frequency of the
 232 fundamental modes excited along the propagation direction is determined by the electrical length (l_e) of
 the cavity. For an air filled waveguide with the relative permittivity $\epsilon_r = 1.0$, $l_e \approx l$.

233



234 **Figure 1 - Microwave cavity test fixture. (1) waveguide, (2) couplers, (3) slot for specimen insertion,**
235 **(4) specimen, (5) specimen holder**

236

237 The specimen is inserted into the cavity through a narrow slot (3) (1 mm x 10 mm), precisely machined
238 through both walls of the waveguide in the centre of the cavity, where the electric field (E) attains a
239 maximum value. The specimen (4) is attached to a stage (5). The stage is used to control and measure
240 the specimen area inside the cavity. In the case of liquid samples the entire test fixture in Figure 1 may
241 be reoriented to perform the measurement of the specimen in horizontal position.

242 **5 Test Specimen**

243 The test specimen consists of a graphene layer coated on or bonded to a non-conducting substrate. The
244 substrate provides mechanical support for handling and positioning the graphene materials inside the
245 test fixture. In order to minimize effects of the substrate on the measurement, the substrate material
246 should exhibit low conductivity and low dielectric permittivity. The recommended substrate for graphene
247 obtained from CVD, exfoliation or other synthetic routes, is electronic grade fused silica wafer, 200 µm to
248 250 µm thick. The graphene material to be tested should be transferred onto the substrate surface using
249 a process that preserves the integrity and purity of the graphene layer, while minimizing the possibility of
250 contamination. The method requires both, the coated and uncoated substrate. The recommended size of
251 test specimen is 3 mm x 20 mm. Epitaxial graphene grown on silicon carbide (SiC) may be tested directly
252 on the native substrate after removing either the Si- or C-terminated face. Epitaxial graphene can be
253 grown by heating the SiC single crystal in under ultra-high vacuum or in an inert gas atmosphere. The
254 SiC surfaces used for graphene growth contain Si- and C-terminated faces. On the Si-face,
255 homogeneous and clean graphene can be grown with a controlled number of layers. The carrier mobility
256 reaches as high as several $\text{m}^2 \text{V s}^{-1}$, although this is reduced by the presence of the substrate steps. On
257 the C-face, although the number of layers is not homogeneous, twisted bilayer graphene can be grown,
258 which is expected to be the technique of choice to modify the electronic structure of graphene (see
259 Clause 9, note 1).

260 **6 Measurement procedure**

261 **6.1 Apparatus**

262 The measurement requires an automatic two port vector network analyser (VNA) operating in the
263 frequency range that covers the X- frequency band (6 GHz to 12 GHz) with the capability of measuring
264 the scattering wave parameters S_{21} or S_{12} transmitted between ports 1 and 2 of the VNA. Connections
265 between the test fixture (Clause 4) and the network analyser should be made using high quality coaxial
266 cables and appropriate adapters. The dynamic range of the measurements should be within 70 dB or
267 greater. The instrument should be equipped with an IEEE 488.3 I/O interface or equivalent, for
268 transferring data between the network analyser and a data collection unit.

269 **6.2 Calibration**

270 Calibration is required only at the coaxial ends. Two-port full calibration for S_{21} and S_{12} should be
271 performed in accordance with the network analyser manufacturer's specification using an appropriate
272 Short-Open-Load calibration kit.

273 **6.3 Measurements**

274 Connect *the empty* test fixture to the vector network analyser (VNA). Set the VNA to measure S_{21}
 275 *magnitude* with 800 *data points* or more. Select the *frequency span* to 2 GHz and the *centre frequency* to
 276 8.5 GHz. Several resonant peaks should appear on the VNA screen, each with the $|S_{21}|$ max value of
 277 about –20 dB and the S_{21} minimum value (noise floor) in the range of –60 dB or less. Identify the
 278 resonant frequency (f_0) of the third resonant peak TE_{103} , for which the electric field of the standing wave
 279 attains its maximum value in the middle of the cavity (see Clause 9, note 2).

280 **6.3.1 Empty Cavity**

281 Set the *centre frequency* to f_0 and the *frequency span* to about $2\Delta f$ (4 MHz or less), such that $|S_{21}|$ peak
 282 height is about 5 dB. Determine the half power bandwidth, $\Delta f = |f_2 - f_1|$, where f_2 and f_1 are frequencies of
 283 the resonant peak, 3dB below the $|S_{21}|$ maximum. Determine the quality factor Q_0 of the *empty cavity*
 284 from equation (1).

$$285 \quad Q_0 = \frac{f_0}{\Delta f} \quad (1)$$

286 **6.3.2 Specimen**

287 Insert the specimen into the cavity in steps (x), while measuring the length of the insertion (h_x) perturbing
 288 the cavity volume (see Clause 9, note 3). Record the area (A_x) of the sample inside the cavity at each
 289 step (x).

$$290 \quad A_x = w \cdot h_x \quad (2)$$

291 where w is the width of the test specimen. When the cavity is perturbed by the specimen, the position (f_x)
 292 of the resonant peak should move to lower frequencies and the $|S_{21}|_{\max}$ value should decrease when A_x
 293 increases. Adjust the *center frequency* and the *frequency span* as in 6.3.1, if necessary. Record the
 294 resonant frequency f_x , half power bandwidth Δf and the corresponding quality factor Q_x (Eq. 1). (See
 295 Clause 9, note 4).

296 **6.3.3 Repeated procedure**

297 Repeat the steps in 6.3.2 recording Q_x and A_x , until $h_x \geq 10$ mm ($h_x \geq a$) or when the resonant peak height,
 298 $|S_{21}|_{\max}$, decreases to about 10 dB above the noise level.

299 **6.3.4 Substrate**

300 Optionally perform steps 6.3.2 – 6.3.3 for bare substrate.

301 **7 Calculations of surface conductance**

302 Equation (3) correlates the specimen surface conductivity with the measured quality factor and the
 303 specimen surface area [4]:

$$\frac{1}{Q_x} - \frac{1}{Q_0} = \sigma_s \frac{2}{\pi \varepsilon_0 f_0 V_0} (w h_x) \quad (3)$$

305 where:

306 σ_s = specimen surface conductance

307 $w h_x$ = specimen surface area inside the cavity

308 Q_x = quality factor of the specimen

309 Q_0, f_0 = quality factor and resonant frequency of empty cavity

310 V_0 = volume of the empty cavity, $V_0 = a \cdot b \cdot l$ (see Fig. 1)

311 ε_0 = permittivity of free space.

312 Since for a given cavity V_0 , Q_0 , and f_0 , are constant parameters (3) can be rearranged into to (4) which
313 can be fitted to a straight line.

$$\frac{1}{Q_x} - \frac{1}{Q_0} = \sigma_s \cdot k (w h_x) \quad (4)$$

315 Where:

316

317 $k = 2 / (\pi \varepsilon_0 f_0 V_0)$.

318 Thus, σ_s can be solved from the slope of a linear portion of plot $(1/Q_x - 1/Q_0)$ vs $(k w h_x)$ (see Figure A2 of
319 Annex A).

320 8 Report

321 The report shall include the following:

322

323 – Preparation procedure and dimensions of the specimen.

324 – Values of V_0 , Q_0 , and f_0 .

325 – Table of f_x , Q_x and h_x for the sample specimen with graphene layer

326 – Plot of $1/Q_x - 1/Q_0$ vs $(k w h_x)$ for the sample specimen containing graphene layer on the substrate.

327 – Table of f_x , Q_x and h_x for the specimen of bare substrate having nominal width w same as the sample
328 specimen.

329 – Plot of $1/Q_x - 1/Q_0$ vs $(k w h_x)$ for the bare substrate.

330 – Measured surface conductance for specimen containing graphene layer on the substrate, σ_{s_m} .

331 – Measured surface conductance for specimen of bare substrate, σ_{s_t} .

332 – The effect of substrate may be neglected if $\sigma_{s_m} \gg \sigma_{s_t}$. In the case if σ_{s_m} value is comparable to σ_{s_t}
333 but σ_{s_m} is larger than σ_{s_t} at least by two orders of magnitude, subtract σ_{s_t} from σ_{s_m} [5].

334 – Report surface conductance, σ_s , for the graphene layer $\sigma_s = \sigma_{s_m} - \sigma_{s_t}$

335 – In the case if $\sigma_{s_m} \approx \sigma_{s_t}$ examine the test specimen preparation procedure (see Clause 9, note 5).

336

337 9 Notes

338 1. From the application point of view, graphene on SiC will be used as a standard reference graphene
339 material and the platform used to fabricate high-speed electronic devices and dense graphene
340 nanoribbon arrays, which will be used to introduce a bandgap [3]

341 2. The electric field inside the cavity attains a maximum value in the middle of the cavity where the
342 specimen is inserted for odd fundamental $TE_{1,0,n}$ modes, where $n= 1,3,5,\dots$. The first resonant mode,
343 $TE_{1,0,1}$, may fall within the waveguide cut-off frequency, below 6.5 GHz, if the cavity is electrically too
344 long. Therefore, the test method recommends to use modes 3,5,7,... These modes can be easily
345 identified. Inserting the specimen into the cavity causes all the resonant peaks corresponding to odd
346 modes to decrease in magnitude and shift to lower frequencies, while the resonant peaks corresponding
347 to even modes ($n=2,4,6,\dots$) remain intact.

348 3. The active length (h_x) perturbing the cavity volume corresponds to the portion of the specimen inside
349 the cavity (see Fig.1-1). The typical value of Q_0 is about 3000, which can be measured with uncertainty
350 $\Delta Q \approx 10$ [5]. Therefore, the minimum insertion h_{x0} which cause the quality factor to change from its initial
351 value Q_0 can be determined experimentally from uQ .

352 4. The operating menu of a typical automatic network analyser includes functions for finding the *peak*
353 *maximum* (resonant frequency), calculating the *half-power* bandwidth, *Q factor*, and for adjusting the
354 *centre frequency* and the *frequency span*. These functions can be executed either manually or invoked
355 from a stored macro program for automated calculation of Q after each specimen insertion step.

356 5. The typical surface conductance value of graphene materials can be between 1 S (for a multilayer
357 and/or doped graphene) and 10^{-5} S (for SGL). Such conductance values are much larger than the typical
358 surface conductance of fused silica substrate and therefore the effect of substrate can be neglected in
359 most cases. When the film consists of a not percolated semi- continuous network of graphene flakes, σ_s
360 can be much smaller than 10^{-5} S. Similarly, σ_s can decreases rapidly with increasing concentration of
361 carbon sp^3 defects, for example, after chemical functionalization or incomplete reduction of rGO. In the
362 case when the measured surface conductance is comparable to surface conductance of the substrate the
363 measurement results may be unreliable. Example measurements are illustrated in Figs A1 and A2 for
364 single layer and multi-layer CVD graphene deposited on a fused silica substrate (see Annex A)

365 10 Accuracy Consideration

366 Several uncertainty factors such as instrumentation, dimensional uncertainty of the test specimen
367 geometry, roughness and impurities contribute to the combined uncertainty of the measurements.
368 Adequate analysis can be performed, however, by using the partial derivative technique for equations (3)
369 or (4) and considering the instrumentation and the experimental errors. The standard uncertainty of S_{21}
370 can be assumed to be within the manufacturer's specification for the network analyzer, about ± 0.01 dB
371 for the magnitude and $\pm 0.5^\circ$ for the phase. The resonant frequency can be determined to within few kHz
372 when collecting 800 data points over the frequency span of $2\Delta f$. The corresponding relative uncertainty of
373 the Q_x factor is then typically below 0.5%. The combined relative standard uncertainty of the
374 measurements is typically better than 6 %. Further improvement in accuracy can be achieved by fitting
375 the resonant peak data to a damped oscillator model, which utilizes both, the magnitude and phase of the
376 measured complex scattering parameter S_{21} [5]. Comparison of calculation techniques for Q-Factor
377 influenced by the measurement uncertainty of the network analyser is given in reference [6].

378 Additional limitations may arise from the systematic uncertainty of the particular instrumentation,
379 calibration standards and the dimensional and structural imperfections of the actually implemented test
380 specimen.

381

382 **Annex A**
383 (informative)

384 **Case study of surface conductance measurement of SL and ML graphene**
385

386 **A.1 General**

387 In this case study, surface conductance of commercially available SL and ML graphene from the CVD
388 process was measured using non-contact resonant cavity (std. R100 (WR 90) waveguide) operating in
389 the 7.2 GHz frequency range. The implemented partial specimen insertion allows precise control of the
390 sample area in the cavity, more data points for fitting and overall better accuracy. The measurements are
391 referenced to resonant frequency in air.

392 **A.2 Cavity Perturbation Procedure**

393 The cavity perturbation by a specimen, having relative complex permittivity, $\varepsilon_r^* = \varepsilon_r' - j\varepsilon_r''$, is given by
394 equations (1) – (3), where (3) accounts for non-uniform fields [4, 5].

395
$$\frac{f_0 - f_r}{f_0} = (\varepsilon_r' - 1) \cdot 2 \frac{V_r}{V_0} - b_r \quad (\text{A1})$$

396
$$\frac{1}{Q_r} - \frac{1}{Q_0} = \varepsilon_r'' \cdot 4 \frac{V_r}{V_0} - 2b_q \quad (\text{A2})$$

397
$$C_V = \frac{2 \int_{V_r} E_r E_0 dV}{\int_{V_0} E_0^2 dV} = b_r + b_q \quad (\text{A3})$$

398 High frequency structure simulator (HFSS) software was employed to solve (A1-A3) numerically under
399 the assumption that the specimen volume, V_r , is small compared to volume of the cavity, V_0 , $V_r \ll V_0$,
400 and the sample permittivity does not depend on V_r . In the range of Q_r , and V_r values where $b_r + b_q =$
401 constant equations (1) and (2) are linear and can be solved for ε_r^* by measuring Q_0 , Q_s , f_0 and f_r as a
402 function of V_r [4]. Inserting into cavity, tuned at the resonant frequency f_0 , a low loss substrate, having
403 permittivity $\varepsilon_{\text{sub}}^* = \varepsilon_{\text{sub}}' - j\varepsilon_{\text{sub}}''$, thickness t_{sub} and volume $V_{\text{sub}} = w t_{\text{sub}} h$, causes the resonant frequency shift
404 to lower frequencies from f_0 to f_{sub} , which is proportional to $\varepsilon_{\text{sub}}'$. The corresponding quality factor
405 decreases from Q_0 to Q_{sub} , which depends on $\varepsilon_{\text{sub}}''$. Similar experiments with nominally the same
406 substrate coated with a conducting layer of graphene material, having permittivity $\varepsilon_G^* = \varepsilon_G' - j\varepsilon_G''$, thickness
407 t_G and volume $V_G = w t_G h$, causes the resonant frequency shift from f_0 to f_G , which is proportional to the
408 effective dielectric constant ε_{Gs}' . The quality factor decreases from Q_0 to Q_{Gs} , due to combined losses of
409 the substrate and the graphene layer, $\varepsilon_G'' + \varepsilon_s''$. The dielectric loss and surface conductance are related
410 by equation (A4):

411
$$\varepsilon_G'' = \frac{\sigma_G}{2\pi\varepsilon_0 f_0 t_G} \quad (\text{A4})$$

412 Assuming that the dielectric loss of graphene is much larger than that of the substrate $\varepsilon_s'' + \varepsilon_G'' \approx \varepsilon_G''$,
413 equation (A2) can be simplified and rearranged into equation (A5):

414
$$\frac{1}{Q_x} - \frac{1}{Q_0} = \frac{\sigma_G}{\pi\varepsilon_0 f_0} \frac{2wh_x}{V_0} - 2b_q \quad (\text{A5})$$

415 where:

416 σ_G = surface conductance of the graphene layer

417 ϵ_0 = permittivity of free space

418 wh_x = area of the graphene layer specimen inserted into the cavity

419 Q_x = quality factor at insertion h_x

420 f_0 , Q_0 and V_0 = resonant frequency, quality factor and volume of the empty cavity respectively.

421 NOTE Equation (A5), from which σ_G is determined, does not depend on the thickness of the graphene layer but on its area, wh_x ,
422 which can be determined with much higher accuracy than t_G .

423 A.3 Experimental

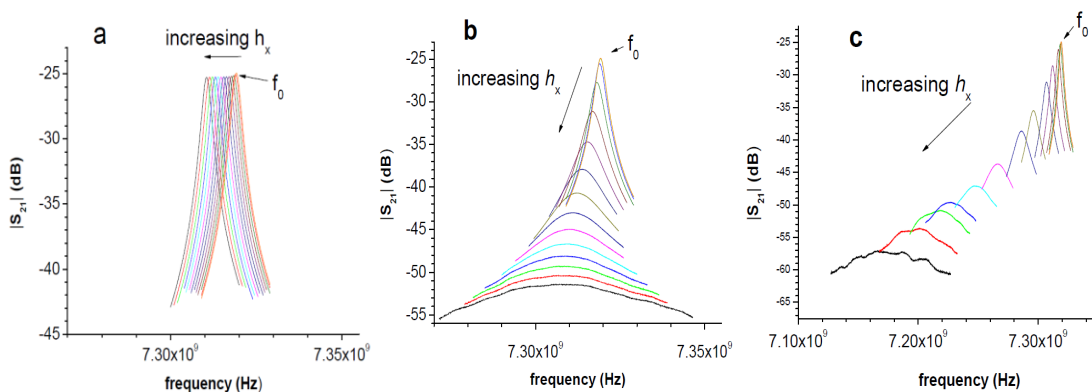
424 Single (SL) and multi-layer (ML) graphene from a CVD process were obtained from a commercial source
425 [6] and transferred on to 200 μm thick fused silica wafers [7], from which 3 mm x 20 mm specimens were
426 extracted by dicing.

427 The cavity test fixture design shown in Figure 1 employs a 134 mm long R100 waveguide operating in the
428 microwave X-band, 6 GHz to 12 GHz [5]. The specimen area inside the cavity is controlled by partial
429 insertion. The fixture is connected to a network analyser (Agilent 8720D) with semi-rigid coaxial cables
430 and coaxial to R100 adapters. The walls of the cavity are implemented via R100 couplers, which are
431 cross-polarized ($\varphi = 87^\circ$) in respect to the waveguide polarization. The system is calibrated at the coaxial
432 ends using a Short-Open-Load calibration kit. The resonant frequency f_x and half power bandwidth Δf_x is
433 determined for each $\text{TE}_{103} - \text{TE}_{109}$ odd resonant modes, from the measured scattering parameter peaks
434 between 6 GHz and 12 GHz. The test fixture, instrumentation and the measurement procedure are
435 described in Clauses 4–8. Here, f_0 of the TE_{103} peak = 7.3191125 GHz, $Q_0 = 3000$ and $V_0 = 33.491 \text{ cm}^3$.

436 NOTE Certain commercial equipment, instruments, or materials are identified in this document in order to specify the procedure
437 adequately. Such identification is not intended to imply recommendation or endorsement, nor does it imply that the materials or
438 equipment identified are necessarily the best available for the purpose.

439 A.4 Results

440 Figure A.1 shows the magnitude of the scattering parameters $|S_{21}|$, at the TE_{103} resonant peak measured
441 for a single and multi-layer graphene, as a function of the specimen insertion into cavity. Figure A.1a
442 shows that with increasing insertion, the height of the resonant peak of fused silica substrate remains
443 relatively unchanged indicating a low conductivity of the substrate, therefore confirming validity of
444 simplifying assumption in equation (5). In comparison, Figure A.1b shows that the height of the resonant
445 peak of SL graphene decreases considerably with increasing specimen insertion due to much higher
446 conductance of the graphene layer. The conductance of ML graphene is larger than that of SL graphene,
447 as evidenced by the rapid decrease in the height of the resonant peak shown in Figure A.1c.



448

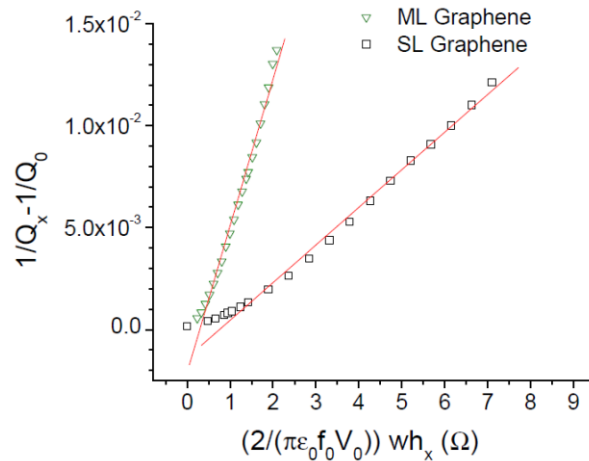
449 Figure A.1 – Scattering parameters $|S_{21}|$ of the resonant peak TE_{103} as a function specimen insertion (h_x),
a-silica substrate, b- single-layer graphene and c- multi-layer graphene.

450 In addition to the decrease in height, this ML resonant peak shifts to lower frequency considerably,
 451 indicating a large dielectric polarization, likely at the boundaries between grains in the ML graphene
 452 sample.

453 A.5 Surface conductance of SL and ML graphene

454 Figure A.2 shows graphical representation of equation (A5), using experimental Q_x and h_x data for SL
 455 and ML graphene, shown in Fig A1. The solid lines are linear fits to equation (A5) through the data
 456 points.

457



458

459 Fig A.2 – Plots of $(1/Q_x - 1/Q_0)$ as a function of the normalized specimen area, wh_x , for (SL) and (ML)
 460 CVD graphene. Symbols represent the data points and lines are linear fits through the points

461

462 The surface conductance, σ_G , is obtained from the slope of the linear portion of the plots where the
 463 parameter b_q in (A5) can be neglected.

464

465 For SL graphene $\sigma_G = 1.84 \times 10^{-3}$ S ($\rho_G = 543$ Ω).

466

467 In the case of ML graphene, $\sigma_G = 7.19 \times 10^{-3}$ S ($\rho_G = 139$ Ω).

468

469 The combined relative uncertainty in σ_G is approximately 1.5%.

470 A.6 Summary

471 The presented surface conductance results qualitatively agree with the published data for similar
 472 graphene materials [8-10], though they may reflect the particular morphologies, density of states and
 473 structural imperfections resulting from the particular CVD process. Graphene material (up to 10 layers) is
 474 considered to be a 2D conductor, for which the surface conductance σ_s is the appropriate measure of its
 475 electrical conduction. Volume conductance of thicker layers can be obtained dividing σ_s by the layer
 476 thickness.

477 The effect of conductivity (and the dielectric constant) of the substrate on the measurement of
 478 conductivity of graphene can be corrected using the procedure described in 8.1.10, and in reference [5].

479

Bibliography

- 480 1. Alcalde, H. ; de la Fuente, J. ; Kamp, B. ; Zurutuza, A., *Market Uptake Potential of Graphene as a Disruptive*
481 *Material*, **Proceedings of the IEEE**, vol. 101, No. 7 (July 2013).
- 482 2. J. Obrzut, *Graphene: a New Horizon for Modern Technology*, NEMA Electroindustry Magazine, page 9,
483 September (2011).
- 484 3. W. Norimatsu and M. Kusunoki, *Semicond. Sci. Tech.* vol. 29, p. 064009 (2014).
- 485 4. J. Obrzut, C. Emiroglu, O. Kirillov, Y. Yang, R. E. Elmquist, *Measurement*, vol. 87, pp. 146-151 (2016).
486
- 487 5. N. Orloff, J. Obrzut et al, *IEEE MTT Transactions*, vol.62, pp. 2149-2158 (2014).
- 488 6. Y. Kato and M. Horibe, *IEICE Trans. Electron.*, vol.E97-C, no.6, June 2014.
- 489 7. <https://graphene-supermarket.com/>
- 490 8. T. Takami, R. Seino, K. Yamazaki and T. Ogino, *J. Phys. D: Appl. Phys.*, vol. 47, p. 094015 (2014)
- 491 9. J. Krupka et al, *Appl. Phys. Lett.* vol. 96, p. 082101 (2010).
- 492 10. L. Hao et al, arXiv:1304.1304 (2013).
- 493 11. Bianco and T. Kyotani, *All in the graphene family- A recommended nomenclature for two-dimensional carbon*
494 *materials*, *Carbon* vol. 65, pp. 1-6 (2013).

495

496